Theoret. Chim. Acta (Berl.) 63, 235–243 (1983)

THEORETICA CHIMICA ACTA

A Study of the Nonadiabatic Effects in the Li–Li_2^+ System: Typical Minimum Energy Paths for the Reaction $Li + Li_2^+ \rightarrow Li_3^+$

Jan Vojtík, Alena Krtková, and Rudolf Polák

J. Heyrovský Institute of Physical Chemistry and Electrochemistry, Czechoslovak Academy of Sciences, CS-12138 Prague, Czechoslovakia

Mutual arrangement and nonadiabatic coupling between the lowest two singlet potential energy surfaces of the Li_3^+ system are studied along typical ground-state minimum energy paths for the reaction $Li + Li_2^+ \rightarrow Li_3^+$. The potentials and nonadiabatic coupling matrix elements are obtained using the diatomics-in-molecules method. The relative Li–Li_2^+ motion along the pathways is predicted to be inefficient in causing nonadiabatic transitions from the ground state to the first excited state of the system.

Key words: Nonadiabatic effects – Minimum energy path.

1. Introduction

Chemical reactions and other elementary processes can be divided into two classes. The first class consists of those processes, during the course of which the electronic motion can be separated from the nuclear one and which are, therefore, governed by a single adiabatic potential energy surface (PES) [1]. There are however an enormous number of processes in which the Born–Oppenheimer approximation breaks down and which, consequently, cannot be pictured as taking place on a single adiabatic PES. Such kinds of processes constitute the second class. Electronically nonadiabatic behaviour has been observed in many gas phase elementary processes, e.g., electronic energy transfer, charge transfer, quenching of electronic excitation etc. [2]. Recently, attention has also been directed towards nonadiabatic effects associated with gas-surface processes, including adsorption on semi-infinite metals [3, 4] and its cluster

---

Offprint requests to J. Vojtík

models [5, 6]. The nonadiabatic behaviour of a system is caused by the nuclear motion and is connected with the occurrence of such mutual arrangements of two or more adiabatic PES's as is their intersection or avoided crossing, and with the existence of such regions of nuclear configuration space where the nonadiabatic coupling matrix elements between the relevant adiabatic wave functions are large [3].

In order to decide whether a system can undergo nonadiabatic transitions, one should ideally have information of this kind on the whole configuration space. Thus, taking into account the dynamical aspect of the problem, one can gain a notion how nonadiabatic effects, if any, will influence behaviour of the system of the reactants not only under normal, chemical conditions, but also in those cases when the reactants prepared in particular internal and translational states are brought together in molecular beam experiments. However, the necessary potential energy surfaces and nonadiabatic coupling are, especially for complex systems, extremely difficult to obtain for the whole configuration space. Therefore, one is often forced to content oneself with information provided by a few cuts through the relevant PES's. Though a picture of the possible nonadiabatic behaviour of the system thus obtained can hardly be expected to go beyond the chemical way of thinking (even in this context the picture must be regarded as rather tentative), it may prove very useful. The correlation diagrams between the reactants and products of the reaction $F+H_2 \rightarrow FH+H$ [8], or cuts through the PES's corresponding to the idealized motion of the adatom to a cluster model of a metal surface [5, 6], may serve as an illustration of this fact.

In the present paper we embark on the study of nonadiabatic effects in the system Li–Li_2^+. Following the "chemical" approach we construct typical ground state minimum energy paths (MEP's) for the reaction $Li+Li_2^+ \rightarrow Li_3^+$ and calculate mutual arrangement of the lowest singlet potentials and nonadiabatic interaction between them along these pathways. Besides the methodical aspect, the study is also of practical interest due to a probable role of this reaction in the processes of lithium cluster formation in molecular beams.

2. Computational Details

The approximations to the true singlet potential energies and nonadiabatic coupling matrix elements were obtained using the semiempirical VB technique of diatomics in molecules (DIM) [9–11] which has turned out to be quite successful in the theoretical investigation of those processes where excited states and their coupling with the ground state (GS) PES play an important role. A minimum basis was taken which arises by including the ^2S ground state and the ionized $Li^+(^1S)$ state on each nucleus [12, 13]. The resulting VB structures lead to three spin adapted singlet polyatomic basis functions. The DIM hamiltonian matrix for the Li_3^+ system is written as

$$\boldsymbol{H} = \sum_{K>L=1}^{3}\sum^{2} \boldsymbol{T}_{(KL)}\boldsymbol{h}^{(KL)}\boldsymbol{T}^{+}_{(KL)} - \sum_{K=1}^{3} \boldsymbol{h}^{(K)}. \tag{1}$$

The transformation matrices $\boldsymbol{T}_{(KL)}$ as well as the spin adapted basis functions were obtained by the direct diagonalization approach [14]. As the basis is composed of only S-type states, the $\boldsymbol{T}_{(KL)}$ matrices are independent of the geometrical configuration of the system. For the evaluation of the (diagonal) elements of the fragment hamiltonian matrices $\boldsymbol{h}^{(KL)}$, ${}^1\Sigma_g^+$ potential energy curve (PEC) of Li_2 and ${}^2\Sigma_g^+$ and ${}^2\Sigma_u^+$ PEC's of Li_2^+ were taken from the work of Pickup [12]. The atomic contributions to the polyatomic hamiltonian matrix were obtained under the usual assumption that the atomic functions, of which the polyatomic basis is composed, are eigenfunctions of atomic hamiltonians.

The diatomic fragment hamiltonian matrices $\boldsymbol{h}^{(KL)}$ of Eq. (1) are diagonal. Therefore, the hamiltonian matrix is, for the present choice of the basis, equal to the $\boldsymbol{S}^{-1}\boldsymbol{H}$ matrix of the nonhermitian formulation of the DIM method [15], which exactly includes overlap into the scheme. Here, with an eye to our need to compute the energy gradient and the nonadiabatic coupling vector, we take the eigenvalues of Eq. (1) as a result of the application of the standard hermitian DIM version with the neglect-of-overlap assumption invoked. Accordingly, the energy gradient was computed in much the same way as in Ref. [13], the nonadiabatic coupling vector

$$\boldsymbol{c}_{ji} = \langle \Psi_j | \nabla \Psi_i \rangle \tag{2}$$

associated with the adiabatic wave functions was approximated, as usual in the DIM scheme [16], by the expression

$$\boldsymbol{c}_{ji} = \boldsymbol{C}_j^+ (\nabla \boldsymbol{H}) \boldsymbol{C}_i / (E_i - E_j), \tag{3}$$

where E_i and $\boldsymbol{C}_i$ are the corresponding eigenvalue and eigenvector, respectively, of the polyatomic hamiltonian matrix (1) and $\nabla\boldsymbol{H}$ is the matrix formed by the gradients of the individual elements of the DIM hamiltonian matrix (1).

3. Construction of Minimum Energy Paths

In what follows, the internuclear distances (ID's) between the individual Li nuclei of the Li_3^+ system are denoted by R_{12}, R_{13} and R_{23}. When the system can be regarded as Li interacting with Li_2^+, then R_{23} is reserved for the ID in this diatomic; d denotes the separation from Li to the centre of mass (c.m.) of Li_2^+, while X signifies cartesian coordinates of the nuclei.

The equilibrium ID for Li_2^+, R_{23}^r, is in our calculation 5.852595 a.u. and the minimum energy of the reactants, E_1^r, is −0.441801 a.u. When all possible orientations of Li_2^+ to Li are taken into account, the Li_3^+ system reaches E_1^r in the region of the configuration space characterized by

$$R_{23} = R_{23}^r, \qquad d \geq 18 \text{ a.u.} \tag{4}$$

i.e. for relatively very large distances d, indicating that the Li–Li_2^+ interaction is of a long-range nature. Obviously, in the region (4), the GS energy satisfies the equation

$$\nabla E_1(X) = 0. \tag{5}$$

The overall minimum on the GS PES is reached for the Li_3^+ system in the D_{3h} configuration with $R_{12}=R_{13}=R_{23}=R^p=5.563614$ a.u. The GS energy corresponding to this minimum, E_1^p, is -0.525005 a.u. [13]. The above given values for E_1^r and E_1^p, along with our sample calculations of the GS energy in the region $R_{23}=R_{23}^r$, 10 a.u. $\leq d \leq 15$ a.u. and the information on the GS PES obtained in our previous study [13] led us to believe that for any initial orientation of the reactants, the MEP is, in all probability, a steepest descent path from the reactants to the product. In such a situation, the construction of the MEP is facilitated by the fact that from any point on the MEP, say X_i, a sufficiently accurate approximation to another point on the MEP, lying in the vicinity of X_i, closer to the product, can be obtained by a translation

$$\delta X_i = -|\varepsilon_i| \nabla E_1(X_i). \tag{6}$$

Here $\nabla E_1(X_i)$ is the gradient of the PES at X_i and $|\varepsilon_i|$ is a sufficiently small parameter. It should be noted, however, that for a successful application of a recursive procedure based on the above property of the steepest descent path, a careful control of the step size (6) is required so as to minimize possible oscillations about the desired MEP.

We chose to construct three MEP's differing in the direction how Li approaches Li_2^+ in the asymptotic region: (1) collinearly, (2) at a 45° angle to the Li_2^+ bond, (3) perpendicularly. Hence, in the asymptotic region, the Li–Li_2^+ system possesses, respectively, $C_{\infty v}$, C_s and C_{2v} symmetries.

In constructing the coordinates, we faced the problem of choosing suitable initial path-limiting structures. This is primarily caused by the fact that there is a relatively large region of the configuration space, given approximately by

$$R_{12}=R_{12}^r, \qquad 15 \text{ a.u.} \lesssim d \lesssim 18 \text{ a.u.}, \tag{7}$$

in which Eq. (5) is no longer satisfied, but the energy gradient is still so small in magnitude that, due to the numerical uncertainties, it is ill-defined. In order to overcome this difficulty, we first constructed the linear synchronous transit pathway [17] for each of the above Li–Li_2^+ approaches. The initial path limiting structure for the MEP was then taken to be a point on the linear synchronous pathway, which lay close to the nearly asymptotic region (7), and at which the magnitude of the GS energy gradient amounted to approximately 10^{-3} a.u. Starting from these initial configurations, the MEP's were obtained in the manner described above. For most parts of these paths it proved sufficient to keep the size of the translation steps (cf. Eq. (6)) at a value of about 0.1 a.u.

4. Results and Discussion

The resulting MEP's, along with the relevant cuts through the lowest two singlet PES's and the magnitude of the nonadiabatic coupling vector, are presented in Figs. 1 and 2. The lower panel in each plot shows the relationships between the ID's along the pertinent pathway.

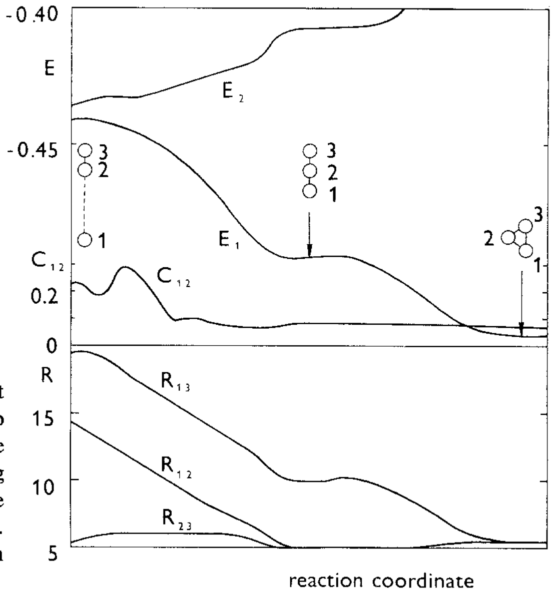

Fig. 1. Ground and first excited singlet PES's along the MEP corresponding to the $C_{\infty v}$ asymptotic structure. C_{12} is the magnitude of the nonadiabatic coupling vector $\boldsymbol{c}_{12}$ along this pathway. The remaining symbols are defined in the text. Distances and energies are measured in atomic units throughout the paper

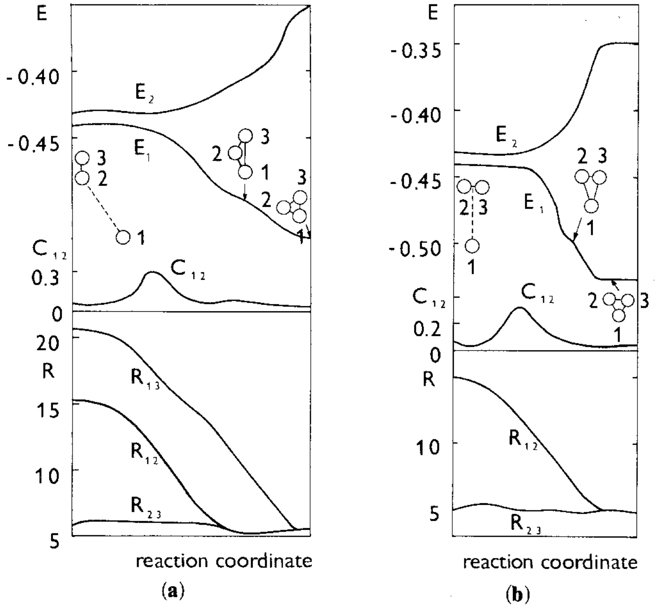

(**a**) (**b**)

Fig. 2a, b. Ground and first excited singlet PES's along MEP's corresponding to initial configurations of (**a**) C_s symmetry, (**b**) C_{2v} symmetry. C_{12} is the magnitude of the nonadiabatic coupling vector $\boldsymbol{c}_{12}$ along the MEP's

In drawing the figures, the independent variable (reaction coordinate) was increased in each iteraction step by the step size δX_i. This quantity was calculated in Cartesian coordinates. As a consequence of numerical inaccuracies in calculating the energy gradient, δX_i may include also such a change in the geometry of the system which corresponds to the motion of the system as a whole (i.e. without varying the ID's). For most parts of the paths, where the energy gradient is substantially different from zero, this spurious contribution to the value of the independent variable is negligible. On the other hand, for those iteration steps where the energy gradient is very small in magnitude, e.g. in the flat region in Fig. 1, the artificial contribution to the step size δX_i (and our independent variable) may be expected to be relatively large. However, in view of the major objective of this paper (study of the nonadiabatic effects), the plots we present are quite satisfactory for the very reason that information on the corresponding changes in the physical space can be deduced from the relationships of the internuclear distances along the pathways.

Vertical cuts through the lowest two PES's along the MEP corresponding to the $C_{\infty v}$ asymptotic structure are shown in Fig. 1. According to the behaviour of the GS energy, the pathway can be divided into two regions. In the first region, the GS energy decreases quite significantly until a critical point on the ground state energy curve is reached, corresponding to the $D_{\infty h}$ configuration of Li_3^+. The basic characteristics of the system in this geometry, summarized in Table 1, indicate that this critical point on the GS PES is a saddle point, even though, due to the symmetry of the system in this geometry, there are two imaginary frequencies corresponding to the negative eigenvalues of the pertinent Hessian matrix. It should be perhaps noted that the existence of this stationary point on the GS PES has not been reported by the previous authors [12, 13, 18]. Returning to the second region of the MEP we note that the system passes the intermediate ($D_{\infty h}$) structure in the direction given by the eigenvector corresponding to the degenerate negative eigenvalues of the Hessian matrix, acquiring C_{2v} symmetry. As it is seen from the lower panel of Fig. 1, this symmetry of the system is, as expected, conserved in the second region of the MEP until the product structure of the D_{3h} symmetry is reached.

Let us now turn our attention to possible nonadiabatic behaviour of the system during the course of the changes in the nuclear configurations corresponding to this MEP. A rough estimate of the transition probability p_{ji} from the state i to the state j can be obtained by using the expression [19, 8]

$$p_{ij} \sim \exp\{-|(E_j - E_i)/\boldsymbol{v}_i \boldsymbol{d}_{ji}|\}. \tag{8}$$

Table 1. Li_3^+ ground state PES-characteristics of the critical point corresponding to $D_{\infty h}$ symmetry

Geometry and energy	Normal modes of vibration j	Frequencies w_j ($Hz \times 10^{13}$)
$R_{12} = R_{23} = R_{13}/2 = 5.16597$ a.u.	1	4.5617
	2	8.3536
$E_1 = -0.492341$ a.u.	3	$6.6735i$
	4	$6.6735i$

Here $\boldsymbol{v}_i$ is the nuclear velocity vector appurtenant to the adiabatic surface E_i and

$$\boldsymbol{d}_{ji} = -i\hbar \boldsymbol{c}_{ji}, \tag{9}$$

the $\boldsymbol{c}_{ji}$ vector having the meaning shown in Eq. (2). At room temperatures, the Li–Li_2^+ relative velocity along the GS MEP cannot exceed a few times 10^{-4} a.u. On the other hand, even in the near asymptotic part of the MEP, where the GS and excited state PES's are relatively close to each other, the magnitude of the nonadiabatic coupling vector is rather small. As a consequence, even in this part of the GS MEP the transition probability is predicted to be negligible. We can therefore conclude that when the idealized Li–Li_2^+ motion corresponding to this MEP is considered, the system is found to behave adiabatically.

The cuts through the lowest two singlet PES's along the MEP obtained for the initial configuration of C_s symmetry are plotted in Fig. 2a. There is a small bump on the GS energy curve located at $R_{23} = R_{12} = 5.217$ a.u. and $R_{13} = 9.576$ a.u., i.e. in the region where the C_s symmetry of the system changes to the C_{2v} one. The corresponding energy is -0.4976 a.u.. As in the previous case, the C_{2v} symmetry, once acquired by the system, is then, with the proviso of the end structure, conserved.

With regard to the validity of the adiabatic approximation along this pathway, the situation is similar to that encountered in the previous case – there is no evidence about the breakdown of the Born–Oppenheimer approximation caused by the nuclear motion corresponding to this pathway.

In Fig. 2b we show the basic characteristics pertinent to the third MEP, which, from the very beginning, corresponds to C_{2v} symmetry. Judging from the first two MEP's, the C_{2v} arrangement of the Li nuclei seems to be favourable for the final stage of the reaction. Accordingly, no change in the symmetry of the system is encountered en route from the reactants to the product. In spite of this, there is a small bump on the ground state energy curve corresponding to the configuration $R_{23} = 5.321$ a.u., $R_{12} = R_{13} = 7.710$ a.u. with energy -0.5004 a.u.. We are therefore tempted to ascribe the existence of the critical points or bumps on the GS energy cuts along our MEP's to a change in the behaviour of the system – from that corresponding to Li interacting with Li_2^+ to a behaviour pertinent to a system where all three Li nuclei began to play almost equivalent role.

Though the reaction coordinate is shorter than in the previous two cases, the basic features with regard to the mutual arrangement of the PES, as well as to the magnitude of the nonadiabatic coupling vector, remain unchanged. This fact indicates that there are no distinct and relatively sudden changes of electronic configuration of the Li_3^+ system caused by the nuclear motion of the system along this MEP which would invalidate the picture of the process based on the Born–Oppenheimer approximation.

Because of the symmetry of the Li – Li_2^+ system, the MEP's constructed in this study can be regarded as representing MEP's for the $Li + Li_2^+ \rightarrow Li_3^+$ reaction quite well. We are therefore led to conclude that the system does not undergo nonadiabatic transitions during an idealized motion along the GS MEP's pertinent to the reaction $Li+Li_2^+ \rightarrow Li_3^+$.

This conclusion may seem rather surprising to anyone acquainted with the results obtained by Preston and Tully [16] in their study on the H^+–H_2 system. These authors calculated the relevant PES's in the whole configuration space and found for asymptotic and nearly asymptotic H^+–H_2 distances very narrow regions with very large nonadiabatic interactions. A close inspection of the situation (and later dynamical study [7]) revealed that the H^+–H_2 system can behave nonadiabatically, provided that the H_2 molecule is initially in at least the fifth vibrational state and/or the relative H^+–H_2 collision energy exceeds 0.072 a.u., i.e., in conditions which can be regarded as "nonchemical". The existence of a strong nonadiabatic coupling between the lowest two PES's was shown to be connected with the symmetry of the H^+–H_2 system. In this respect both systems (H^+–H_2 and Li–Li_2^+) are similar. In view of this feature of the Li–Li_2^+ interaction, the present results should be interpreted so that the MEP's for the reaction $Li+Li_2^+ \rightarrow Li_3^+$ do not pass the pertinent nonadiabatic regions. As in the H^+–H_2 case, these regions should occur at (nearly) asymptotic Li–Li_2^+ separations and the relevant nonadiabatic transitions are to be caused by the vibrational motion of the Li_2^+ diatomic, i.e., the type of motion which obviously does not correspond to the Li–Li_2^+ motion along the MEP's. At present it is impossible to decide whether the situation is similar to that in the H^+–H_2 system or whether our results indicate a serious failure of the crude approach to qualitatively describe the nonadiabatic behaviour of the system exposed to usual chemical conditions. A satisfactory answer to this question can be reached by means of a thorough analysis of the nonadiabatic regions and subsequent determination of those translational and inner states of the reactants which will lead to the nonadiabatic behaviour of the system. A work along this line is in progress.

References

1. Nikitin, E. E.: Adv. Quantum. Chem. **5**, 135 (1970)
2. Tully, J. C. in: Dynamics of molecular collisions, ed. Miller, W. H., part B, Chap. 5, p. 217. New York: Plenum Press, 1976
3. Brivio, G. P., Grimley, T. B.: J. Phys. **C10**, 2351 (1977); Surface Sci. **89**, 226 (1979)
4. Brako, R., Newns, D. M.: Solid State Commun. **33**, 713 (1980)
5. Vojtík, J., Fišer, J., Polák, R.: Chem. Phys. Letters **80**, 569 (1981)
6. Vojtík, J., Fišer, J.: Surface Sci. **121**, 111 (1982)
7. Tully, J. C., Preston, R. K.: J. Chem. Phys. **55**, 562 (1971)
8. Faist, M. B., Muckerman, J. T.: J. Chem. Phys. **71**, 233 (1979)
9. Ellison, F. O.: J. Am. Chem. Soc. **85**, 3540 (1963)
10. Tully, J. C.: J. Chem. Phys. **58**, 1396 (1973)
11. Steiner, E., Certain, P. R., Kuntz, P. J.: J. Chem. Phys. **59**, 47 (1973)
12. Pickup, B. T.: Proc. Roy. Soc. **A333**, 69 (1973)
13. Polák, R., Vojtík, J., Schneider, F.: Chem. Phys. Letters **53**, 117 (1978)
14. Vojtík, J., Paidarová, I.: Chem. Phys. Letters **91**, 280 (1982)
15. Tully, J. C., Truesdale, C. M.: J. Chem. Phys. **65**, 1002 (1976)
16. Preston, R. K., Tully, J. C.: J. Chem. Phys. **54**, 4297 (1971)

17. Halgren, T. A., Lipscomb, W. N.: Chem. Phys. Letters **49**, 225 (1977)
18. Pfeiffer, G. V., Ellison, F. O.: J. Chem. Phys. **43**, 3405 (1963)
19. Tully, J. C.: J. Chem. Phys. **59**, 5122 (1973)

Received December 16, 1982/January 31, 1983